멤브레인(Membrane Journal)
Vol.13, No.3 March, 2003, 131-142

총 설

회전 역삼투 분리막 여과

이 상 호† · Richard M. Lueptow*

한국건설기술연구원 건설환경부, *Department of Mechanical Engineering, Northwestern University

(2003년 8월 5일 접수)

Rotating Reverse Osmosis Membrane Filtration

Sangho Lee† and Richard M. Lueptow*

Construction Environment Research, Korea Institute of Construction Technology, Gyenggi-Do, 411-712, Korea
*Department of Mechanical Engineering, Northwestern University, Evanston, IL, 60208, U.S.A.

(Received August 5, 2003)

요 약: 원통형 회전 역삼투법은 높은 전단력과 유체의 불안정성을 결합시켜 막오염을 감소시키는 동적 여과방법이다. 이 논문은, 회전여과의 물리적 특성, 물질전달과 농도분극 현상, 이론적 및 실험적 해석, 사례연구 등 회전역삼투법에 대한 최근의 연구를 요약해서 보여준다.

Abstract: Cylindrical rotating reverse osmosis (RO) is a means of dynamic filtration that incorporates both high shear and flow instabilities to reduce membrane fouling. This article summarizes recent works on rotating RO including the physics of rotating filtration; mass transfer and concentration polarization; theoretical and experimental analysis; and some case studies.

Keywords: *reverse osmosis (RO), rotating filtration, concentration polarization, fouling*

1. Introduction

Reverse osmosis (RO) filtration has been considered a promising technology for water and wastewater treatment. RO filtration removes ions and organic chemicals, and its treatment efficiency and performance are stable and predictable. RO processing has been successfully applied in desalination of seawater [1]; drinking water production [2], and wastewater recycling in many industries [3-5].

However, a problem that needs to be resolved in the application of RO membranes is the sensitivity to fouling, which results in a decrease in filtrate flux. Concentration polarization and subsequent membrane fouling are the most serious obstacles that limit the acceptance of RO membrane treatment. Therefore, techniques to control membrane fouling are of great importance.

The reduction and alleviation of concentration polarization in filtration and RO have been the focus of much research and development [6]. Attempts to reduce concentration polarization include increasing the fluid velocity [7], inserting turbulence promoters in the feed channels [8], pulsing the feed flow over the membrane [9], and designing the flow path so Dean vortices occur [10,11]. High shear membrane filtration systems such as rotating disk membranes [12] and rotating cylinder filtration [13] have been also investigated because of their potential for reducing polarization.

Among various antifouling techniques, cylindrical rotating filtration that takes advantage of centrifugal

†주저자(e-mail : s-lee@kict.re.kr)

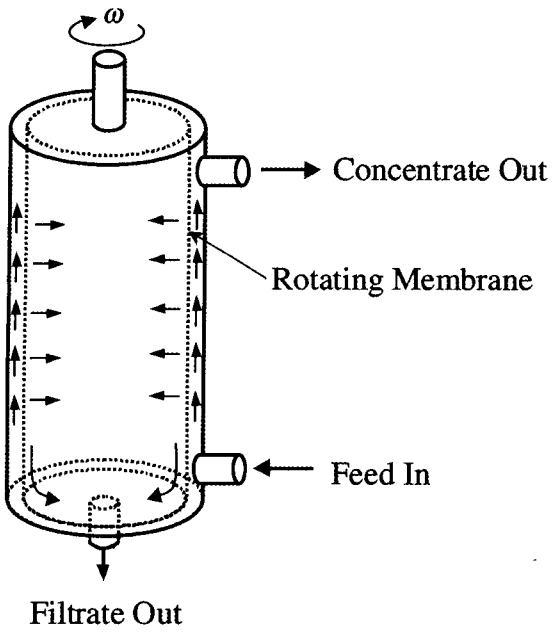

Fig. 1. Schematics of rotating membrane systems.

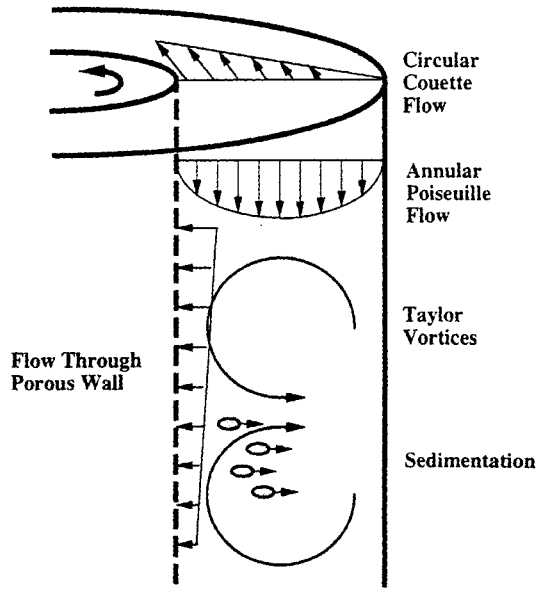

Fig. 2. Sketch of the types of flows that occur in a rotating filter separator.

flow instabilities has drawn attentions as a new technique to control flux decline due to plugging of the filter pores during microfiltration and ultrafiltration. The system consists of a cylindrical filter rotating within a stationary cylindrical shell (Fig. 1). A suspension enters one end of the annulus between the coaxial cylinders and travels axially in the annulus. The permeate passes through the porous inner cylinder and is channeled to the hollow shaft supporting the inner cylinder where it exits the device. The suspension becomes increasingly concentrated as it moves along the annulus to the exit at one end of the annulus. The resulting two products of the device are the concentrated suspension and the particle-free filtrate. The unique advantage of a rotating membrane filtration is that the build-up of particles and other species near the filter surface is very slow compared to dead-end or crossflow filtration [14]. Many studies report a strong anti-fouling effect for rotating microfiltration [15,16] and ultrafiltration [17]. However, relatively little work has been done to further the application of rotating membrane filtration except for blood filtration [18-20] and biological separation [21].

Recently, rotating system for RO has been developed and investigated to control concentration polarization and membrane fouling for improved flux and rejection [22-26]. Rotating RO system has been initially developed for recycling space mission wastewater for long-term space mission such as mission to Mars [27-30] although the technology may be used for most terrestrial RO applications. This article will review the physical basis for rotating filtration and describe recent work to apply it to RO.

2. Physics of Rotating RO

Rotating RO is similar to crossflow RO in that the mean flow is parallel to the filter surface, but the dynamics of rotating RO add forces that tend to keep the suspension species away from the membrane surface. These forces arise from the flow field that results when a membrane on an inner cylinder rotates within a fixed outer cylinder. The flow in the annulus of a rotating RO consists of a superposition between the cylinders, circular Couette flow around the axis of the membrane device, radial flow through the inner cylinder, and centrifugal sedimentation.

These flows are shown schematically in Fig. 2. The

axial annular Poiseuille flow carries the fluid through the device. The circular Couette flow provides a relatively high shear, like that in cross-flow filtration, to wash off the surface of the membrane. Since particles and colloids are typically more dense than the fluid phase of the suspension, the centrifugal acceleration felt by the particles and colloids causes them to sediment away from the filter and outward toward the outer cylinder. Another effect that may contribute to the efficient performance of the rotating RO is the presence of supercritical Taylor vortices, a secondary flow consisting of counter-rotating pairs of toroidal vortices stacked in the annulus and shown schematically in Fig. 3. Taylor vortex flow results from a centrifugal instability and occurs when the speed of the inner cylinder exceeds a critical value. Between the counter-rotating pairs of vortices are strong, jet-like radial outflow regions that tend to accelerate the particles toward the outer cylinder.

In Taylor-Couette flow devices including rotating RO, supercritical circular Couette flow appears as counter-rotating, toroidal vortices stacked in the annulus and superimposed on the stable solution [31]. The appearance of the vertical instability depends upon a dimensionless parameter known as the Taylor number, $Ta=r_i \omega d/\nu$ where r_i is the radius of inner cylinder, ω is the rotational speed, $d = r_o-r_i$ is the gap width, r_o is the radius of outer cylinder, and n is the kinematic viscosity. The transition from stable Couette flow to the vortical Taylor-Couette flow occurs when the Taylor number exceeds a critical value (Ta_c). This phenomenon has been studied from both theoretical and experimental standpoints. Taylor [31] first conducted a simple flow visualization experiment to confirm his analytic prediction for the onset of the instability. Chandrasekhar [32], DiPrima and Swinny [33], Kataoka [34], and Koschmeider [35] provide extensive summaries of the abundant research on this topic since Taylor's pioneering work. A simple and practical way to estimate Ta_c in rotating RO system is to use a modified form given by Murase et al [13] that matches analytical results of Recktenwald et al [36]:

$$Ta_c = 41.02(d/r_i)^{-0.5} + 25.75(d/r_i)^{0.5} + 1.85(d/r_i)^{1.5} \quad (1)$$

This expression matches the analytical value for Ta_c to within 0.5% over all radius ratio, $\eta = r_i/r_o$. Beyond the first transition to Taylor vortex flow, additional flow modes including wavy vortex, turbulent wavy vortex, and turbulent vortex exist [37-39]. DiPrima and Swinney [37] have compiled a summary of experimental results to show that turbulence typically appears above values of Ta/Ta_c greater than 10-12 for radius ratios between 0.8 and 1.

Although several researchers have conducted experi-

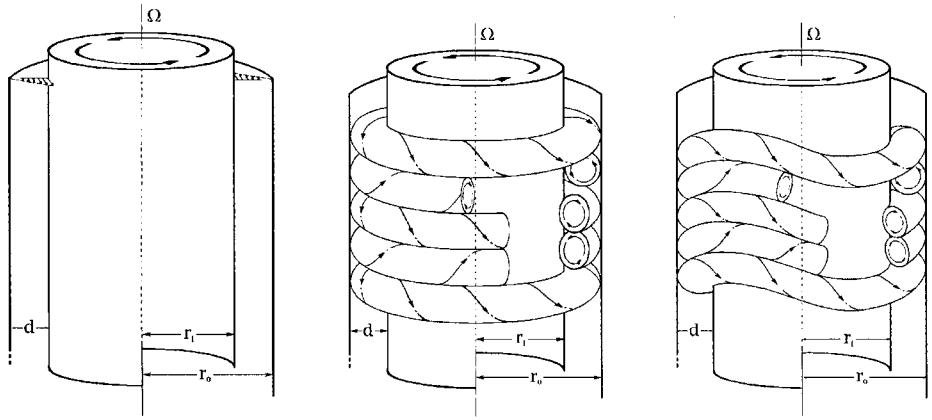

(a) Stable flow (b) Laminar vortex flow (c) Wavy vortex flow

Fig. 3. Flow patterns between rotating concentric cylinders.

ments related to rotating filtration [10,11,13,15-17,40, 41,42], the relative importance of the shear due to the rotation of the inner cylinder, the sedimentation of particles, and the secondary motion of the Taylor vortices to the effectiveness of a rotat ing filtration has not been studied prior to the works by Werely et al [43], Akonur and Lueptow [44] and Schwille [45]. Recent measurements using Particle Image Velocimetry (PIV) revealed that the redistribution of azimuthal momentum by the vortices enhanced the rotational shear in rotating filtration [43,44]. This high rotational shear supplemented by the shear due to the axial flow and centrifugal sedimentation appears to be the key factor in preventing fouling [45]. The rotational shear also reduces the degree of concentration polarization at the surface of the RO membrane, allowing high flux and rejection in rotating RO [22,23,26].

3. Mass Transfer and Concentration Polarization in Rotating RO

Concentration polarization is defined as the accumulation of excess solutes and particles in a thin layer adjacent to the membrane surface. Concentration polarization is inherent of all membrane processes, resulting in an increased resistance to solvent flow and a reduction in permeate flux. The difference between the solute concentration at the membrane, $C_{m,i}$, and the solute concentration in the bulk solution, $C_{b,i}$, originates from the concentration polarization phenomenon. On the basis of the film model theory and from Fick's law for diffusion, the concentration profile near the membrane surface is [18,46]:

$$\frac{C_{m,i}-C_{p,i}}{C_{b,i}-C_{p,i}}=e^{\frac{J_v}{k_i}} \tag{2}$$

where k_i is the mass transfer coefficient for the back diffusion of the solute i from the membrane to the bulk solution on high pressure side of membrane; J_v is the solvent flux, and $C_{p,i}$ is the solute concentration in the permeate [47]. Thus, the growth of the concentration boundary layer is determined by the mass transfer coefficient, k_i , which in turn depends on the axial and rotational motion of the fluid.

Many researches have experimentally and theoretically investigated the radial mass transfer in Taylor-Couette flow. Generally, the mass transfer equations in Taylor-Couette flow satisfy the relation [48]:

$$Sh=A[\,Ta(d/r_i)^{1/2}]\ {}^{a}Sc^{b} \tag{3}$$

where $Sh=2k_id/D$ is the dimensionless mass transfer rate (Sherwood number), $Sc=\nu/D$ is the Schmidt number, D is the diffusion coefficient of the solute, and A, a, b are the constants [17,49]. Most previous studies of mass transfer for rotating systems conclude that A=0.4~1.1, and a=0.4~0.7 under vortical flow conditions. However, most results in the literature were for measurements of the mass transfer coefficient for filtration of suspensions in a cylindrical porous rotating cell or the transport of a chemical species in a cylindrical chemical reactor with a nonporous inner cylinder. Lee and Lueptow [26,50] have measured the mass transfer coefficients in rotating RO and compared them with the results in literature. Using a rearranged form of Eqn (4), the mass transfer coefficients were estimated based on a relatively simple experiment where the permeate flux, applied pressure difference, bulk solute concentration, and permeate concentration are measured [26]:

$$k_i=\frac{J_v}{\ln\left(\frac{1}{RT}\left(\triangle P-\frac{J_v}{L_v}\right)\right)/(C_{b,i}-C_{p,i}))} \tag{4}$$

where R is the gas constant, T is the temperature, ΔP is the transmembrane pressure, and L_v is the solvent transport parameter of the membrane. They provided two different correlations depending on the flow regimes:

$$\mathrm{Sh}=2.15[\,Ta(d/r_i)^{1/2}]^{0.18}\,Sc^{1/3}\ \text{for non-vortical flow} \tag{5}$$

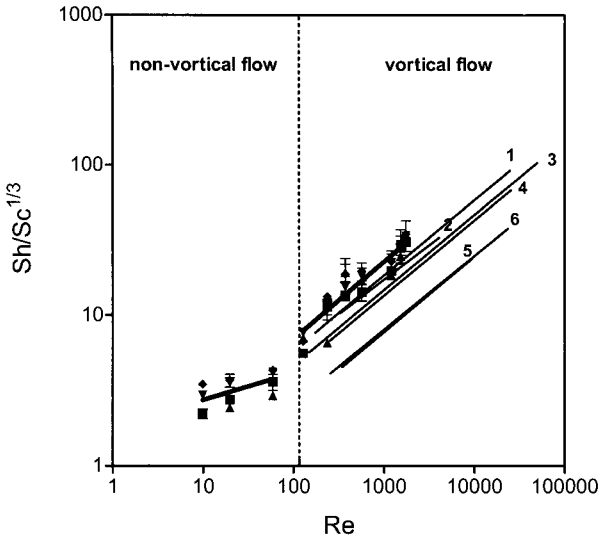

Fig. 4. Mass transfer correlations in rotating RO. (reproduced from [26]) Filled symbols indicate the experimental data. Error bars are smaller than the symbol size except in cases where error bars are shown. Bold lines indicate a least squares fit. (■: NaCl, 6 atm; ▲: NaCl, 8 atm; ▼: NaCl, 10 atm; ◆: Na_2SO_4, 10 atm). 1. Holeschovsky and Cooney [17], 2. Baier [48], 3. Mizushina [51], 4. Kawase and Ulbrecht [53], 5. 'Coeuret and Legrand [52], 6. Kataoka, Doi, and Komai [34]

$$Sh = 1.05[\, Ta(d/r_i)^{1/2}]^{0.18}\, Sc^{1/3} \quad \text{for vortical flow} \quad (6)$$

Fig. 4 shows the dependence of the experimentally measured mass transfer coefficient, represented as $Sh/Sc^{1/3}$, on the Taylor number. The Sherwood number increases with Taylor number as the rotational shear increases. In addition, the Sherwood number jumps to a higher value at the transition from non-vortical to vortical flow as the vortices redistribute azimuthal momentum leading to a higher shear and better mass transfer [26]. The thick solid lines through the data indicate the least squares fit for each flow regime corresponding to the following equations. Fig. 4 also compares the results for rotating RO with previous studies for rotating systems (but not for rotating RO) using various methods including electrochemical methods for non-porous inner cylinders [34,51,52], an ultrafiltration system [17,40], a helical-tube analogy [53], and a theoretical model based on the boundary layer theory [48,49]. The Sherwood numbers measured for rotating RO are slightly higher than those for other rotating systems, although the trend is consistent with previous measurements in different systems. Table 1 summarizes mass transfer correlations in Taylor-Couette flow devices including rotating RO.

Table 1. Summary of the estimations for the mass transfer in various Taylor-Couette flow devices

Method for Measurement	A	a	b	r/d_i	Re_{ax}	$Ta(r/d_i)^{1/2}$	Sc	Ref.
Electrode	0.21	0.7	1/3	0.79	0	>48500	770-8000	[61]
Electrode	0.38	0.5	1/3	0.143, 0.286	30-300	135-1600	1380-6450	[52,62]
Electrode	0.59	0.5	1/3	0.429	30-300	700-3700	1380-6450	[52,62]
Electrode	0.42	0.5	1/3	0.286	30-300	280-1800	1380-6450	[52,62]
Electrode	0.43	0.49	1/3	0.62	0	100-9200	3000-800000	[34]
Electrode	0.12	0.7	0.356	0.7-5.94	0	1600-160000	835-11490	[63]
Electrode	0.74	0.5	1/3	0.62, 0.82	0	59-19500	3000-770000	[51]
Falling film	0.58	0.52	1/3	0.15	140-2600	200-2000	1.74	[64]
Falling film	0.19	0.7	1/3	0.312	33-100	200-680	1260	[65]
Gas reactor	0.46	0.482	1/3	0.62	0-50	650-1950	-	[66]
Gas reactor	0.13	0.72	1/3	0.095	2-200	40-2000	350-420	[67]
Ultrafiltration	0.07	0.62	1/3	0.143	150	450-3500	17000	[40]
Ultrafiltration	0.93	0.5	1/3	0.04-0.148	25-300	68-9740	21600	[17]
Theoretical Analysis	1.65	2/3	1/3	-	-	-	>>1	[48,49]
Theoretical Analysis	1.1	0.46	1/3	0.143, 0.286, 0.429	0	130-1600	>>1	[48,49]
Theoretical analysis	0.68	1/2	1/3	-	0	100-1000	> 10	[53]
RO (vortical flow)	1.05	0.51	1/3	0.153	-	-	-	[26]
RO (non-vortical flow)	2.15	0.18	1/3	0.153	-	-	-	[26]

4. Analysis of Rotating RO System

Few works have been done to analyze the characteristics of rotating RO systems prior to recent studies by Lee and Lueptow [22-24]. They applied the solution-diffusion model modified with the concentration polarization theory to theoretically predict the performance of rotating RO over a wide range of conditions. In the solution-diffusion model, the solvent flux, $J_v(x,t)$, and the flux of solute component i, $J_{s,i}(x,t)$, through the inner cylinder membrane are [18,46]:

$$J_v = L_v(\triangle P - P_{loss}) \tag{7}$$

$$J_{s,i} = J_v C_{p,i} = L_{s,i}(C_{m,i} - C_{p,i}) \tag{8}$$

where L_s is the solute transport parameter and $P_{loss}(x,t)$ is the pressure loss by osmotic pressure and hydrodynamic effects in the annulus. P_{loss} in a rotating RO membrane system with axial flow includes four terms:

$$P_{loss} = \sum_{i}^{n} \triangle \Pi_i + \triangle P_{rot} + \triangle P_{axis} + \rho g x \tag{9}$$

where $\Delta\Pi_i$ (x,t) is the osmotic pressure difference for solute i, ΔP_{rot} is the pressure drop across the annulus gap in the rotating membrane module, ΔP_{axis} is the pressure drop caused by axial flow in the annulus, and gx is the hydrostatic pressure. The osmotic pressure is calculated by Van't Hoff's equation [54]:

$$\triangle \Pi_i = (C_{m,i} - C_{p,i})RT \tag{10}$$

For the conditions in rotating RO, ΔP_{rot}, ΔP_{axis}, and ρgx are negligible compared to $\Delta\Pi_i$ [23].

Rearranging Eqn (2), the equation for concentration polarization effect, the solute concentration at the membrane surface ($C_{m,i}$) can be estimated from the solute concentration in the bulk phase, the permeate concentration, and the water flux. During the filtration, J_v, $C_{b,i}$, and $C_{p,i}$ depend on axial position and time. From a mass balance of solute i, the time rate of change in $C_{b,i}$ in an annular fluid element is given by

$$\frac{\partial C_{b,i}(x,t)}{\partial t} = -\frac{1}{S_a}\left(Q_{conc}(t) + 2\pi r_i \int_x^L J_v(x,t)\,dx\right) \times \frac{\partial C_{b,i}(xt)}{\partial x} + \frac{2\pi r_i \cdot J_v(x,t)}{S_a} C_{b,i}(x,t) - \frac{2\pi r_i \cdot J_{s,i}(x,t)}{S_a} \tag{11}$$

In Eqn (11), $S_a = \pi(r_0^2 - r_i^2)$ is the cross-sectional area of the annulus, and Q_{conc} is the concentrate flow rate. The left hand side is the change in concentration of solute i in the fluid element. The first two terms on the right hand side are the changes in concentration due to axial flux of solute. The last term is the change in concentration due to the flux of solute through the membrane. This model does not account for flow effects near the inlet or outlet, which are negligible based on previous experience with rotating filtration devices [27-32]. The initial condition is that the bulk concentration in the annulus equals the constant inlet concentration so $C_{b,i}(x,0) = C_{b,i}(0,t) = C_{f,i}$ where $C_{f,i}$ is the solute concentration of the feed. By simultaneously solving Eqn (2), (5), (6), and (7)-(11) for a given geometry, the flux and solute concentrations can be calculated as functions of time and axial position [23]. The theoretical model provides insight into the filtration characteristics of rotating RO. The flux and solute rejections from model calculation are shown in Fig. 5 as functions of time. Although the pure water flux of the membrane is 130 L/m^{2}hr, the permeate flux is substantially less because of the high osmotic pressure near the membrane. The flux decreases quite quickly as filtration proceeds because of the rapid increase in osmotic pressure as solute builds up in the annulus [22,23]. The solute rejections are initially high and decrease slightly with time.

The local permeate flux profiles for Fig. 5 at different times are shown in Fig. 6. Initially the flux is uniform, but the flux quickly drops off at the downstream end of the device because of the higher solute concentration there [23]. The difference in flux

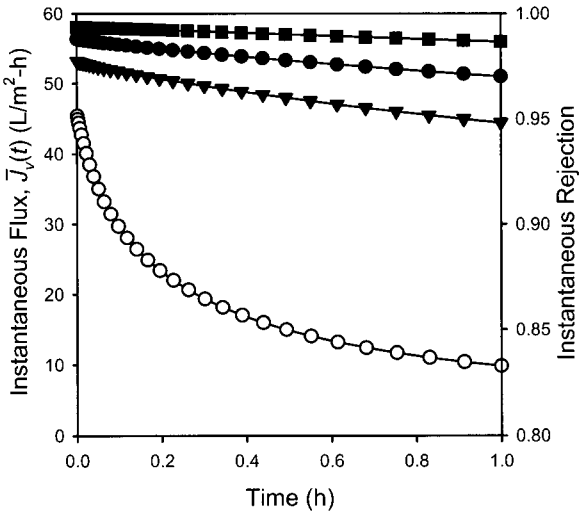

Fig. 5. Variation of permeate flux and rejection with time for space mission wastewater in a rotating RO system. (reproduced from [23]) Modeling condition: ΔP= 1800 kPa; w= 32 rpm (Ta/Ta$_c$=2.54). (○: Flux; ■: Detergent rejection; ●: Nitrogen Rejection; ▼: NaCl rejection)

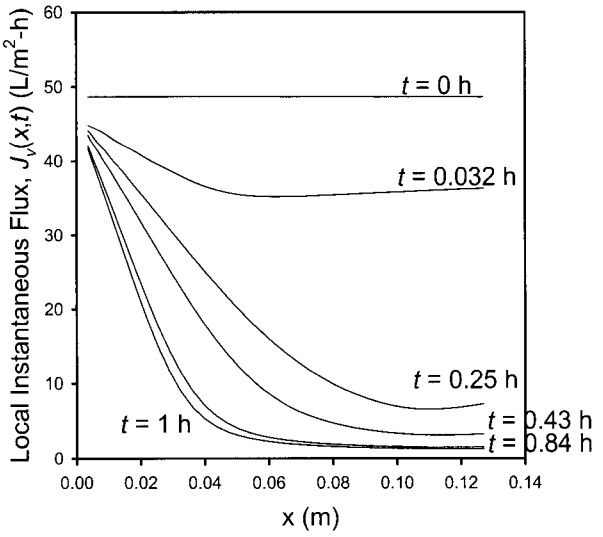

Fig. 6. Local flux profiles of permeate for Figure 5 as a function of time and position. Modeling condition: ΔP= 1800 kPa; ω= 32 rpm (Ta/Ta$_c$=2.54). (reproduced from [23])

between the upstream and downstream ends increases with increasing in time. It is evident that membrane fouling occurs first at the downstream end of the module because of the high solute concentration.

Using a synthetic wastewater, Lee and Lueptow [24, 26] investigate the performance of rotating RO

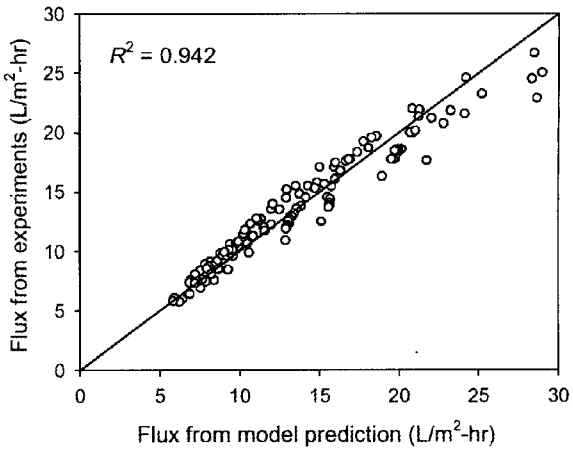

Fig. 7. Comparison of model predictions with experiments. Conditions: ΔP= 600, 800, 1000 kPa; ω=7.5, 15, 90, 180 rpm; 0, 0.2, 0.5, 1, 2.5 mL/min. (reproduced from [57])

experimentally for a wide range of operating parameters and verified the theoretical model for rotating RO. They used a lab-scale test system to measure filtration characteristics for rotating RO. As illustrated in Fig. 7, the model matches the experimental results quite well.

The geometry of the device would be expected to play a role in the effectiveness of rotating RO. A narrow gap (η near 1) would result not only in a high shear but also in a higher critical Taylor number for the appearance of vortical flow. The dependence of permeate flux and solute rejection on the radius ratio, $\eta = r_i/r_o$, was theoretically investigated by Lee and Lueptow [23] as shown in Fig. 8. To change from 0.87 to 0.96, r_i is adjusted keeping r_o constant at 0.0286 m. The flux and rejection decrease with an increase in η except for 0 rpm where the flux and rejection increase. For nonzero rotation, the results can be attributed to the dependence of annulus volume on η. Larger η results in a smaller annulus volume that makes rate of increase in concentration in the annulus faster leading to lower flux and rejection. At 0 rpm, however, the annulus volume effect is negligible because of the high concentration polarization. Instead, an increase in η results in an increasing axial shear because of the narrower annular gap. This shear is negligible in dynamic filtration cases compared to the rotational shear. The sudden drops in flux for vortical

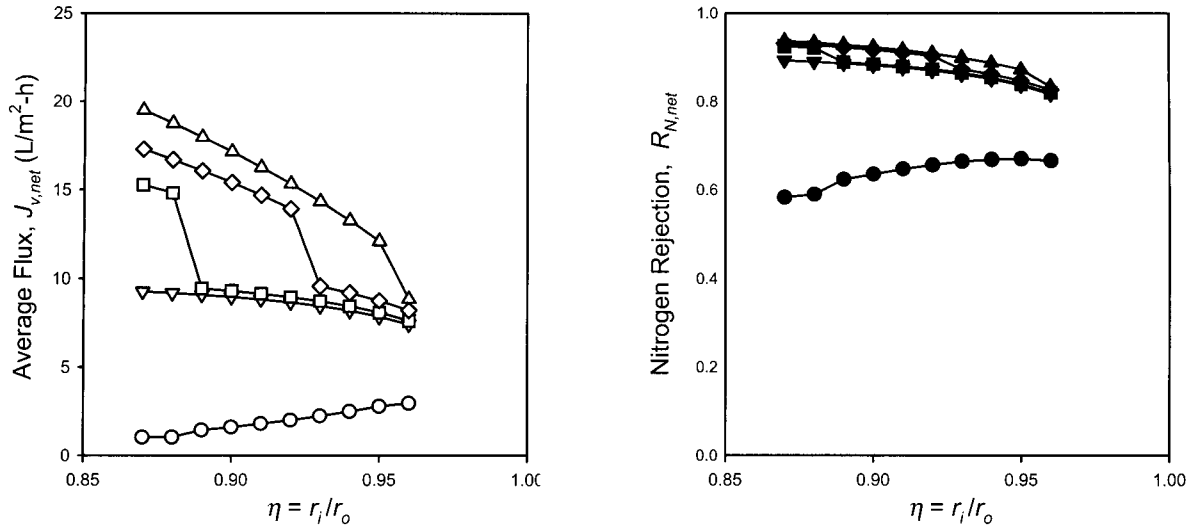

Fig. 8. Effect of radius ratio on flux and total nitrogen rejection in a rotating RO system. Modeling condition: ΔP= 1800 kPa; operating time, 1 hour. (reproduced from [23]) (a) Flux (○: Ta/Ta$_c$ = 0 (0 rpm); ▽: Ta/Ta$_c$ = 0.9 (70.8 rpm); □: Ta/Ta$_c$ = 1.1 (86.5 rpm); ◇: Ta/Ta$_c$ = 2.0 (157.3 rpm); △: Ta/Ta$_c$ = 4.0 (314.6 rpm)), (b) Total Nitrogen Rejection (●: Ta/Ta$_c$ = 0 (0 rpm); ▼: Ta/Ta$_c$ = 0.9 (70.8 rpm); ■: Ta/Ta$_c$ = 1.1 (86.5 rpm); ◆: Ta/Ta$_c$ = 2.0 (157.3 rpm); ▲: Ta/Ta$_c$ = 4.0 (314.6 rpm))

flow (Ta/Ta$_c$ of 1.1, 2.0 and 4.0) can be attributed to the stability of Taylor vortices. The critical Taylor number increases with increasing η. The sudden drops in flux correspond to the radius ratio at which the flow changes from vortical to non-vortical at that rotational speed. The magnitude of the drop in the flux is indicative of how important vortical flow is to enhancing the flux. Unlike the radius ratio, the aspect ratio (r_i/L) of the module does not affect the performance of rotating RO [23].

In addition to the geometric parameters, operating conditions including concentrate flow rate, transmembrane pressure, and rotational speed play an important role in rotating RO membrane performance. In Fig. 9, contours of constant flux and total ion rejection are shown as functions of rotational speed and transmembrane pressure. As expected, the best flux and rejection occur at high rotational speeds and high transmembrane pressures. However, dependence of flux and rejection on rotational speed and transmembrane pressure is not linear. The flux and rejection are suddenly increased at ω = 9.26 rpm because of the flow transition from non-vortical flow to Taylor vortex flow [55]. An increase in the transmembrane pressure results in higher flux and rejection for both non-vortical flow and Taylor vortex flow conditions, but the effect depends on the rotational speed [56]. Thus, increasing transmembrane pressure and rotational speed enhances flux more than simply increasing the rotational speed alone.

The concentrate flow rate (Q_{conc}) also affects the flux and rejection. Flux and rejection increase as the Q_{conc} increases because the high flow rate washes solute out of the device [24,26]. However, Q_{conc} also affects the recovery of permeate. The recovery decreases with an increased Q_{conc} because more fluid is washed out of the system instead of being forced through the membrane [26]. Thus, it is important to increase transmembrane pressure as the concentrate flow is increased to ensure high flux as well as high recovery.

5. Summary

Rotating RO offers breakthrough technology for controlling concentration polarization and membrane

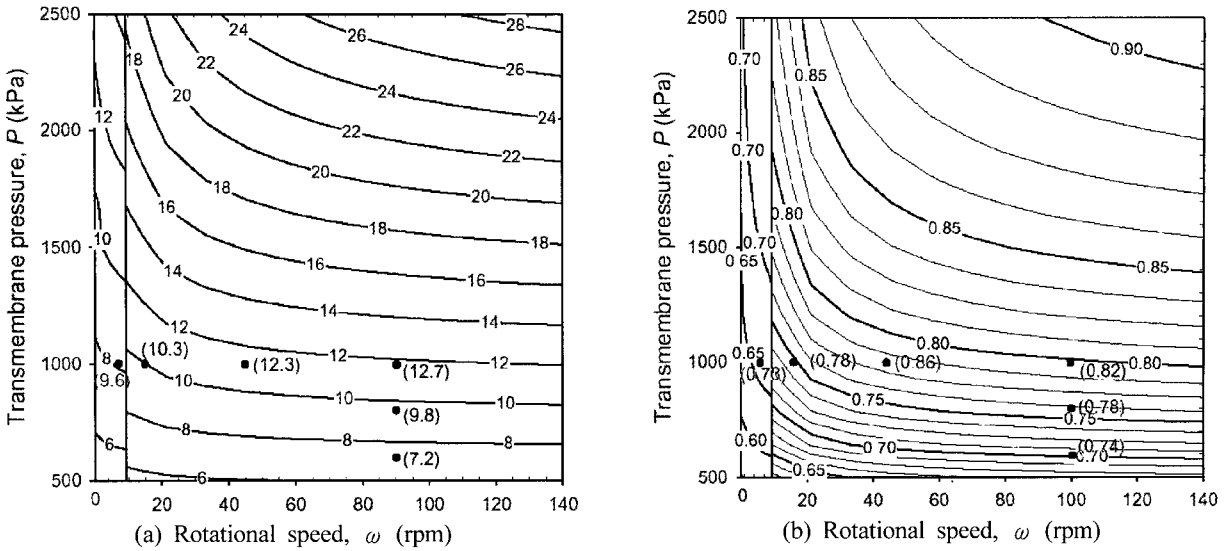

Fig. 9. Contours of time-averaged flux and total ion rejection at different pressures and rotational speeds. (reproduced from [57]) The symbols correspond to data from the experiments with the numerical value of the flux or rejection next to the data point.

fouling, which are major obstacles in applying conventional RO techniques. The unique hydrodynamic features based on the centrifugal instability result in enhanced transport of contaminants away from the RO membrane surface, reducing the accumulation of solute near the membrane surface and the subsequent flux decline. This novel technology holds great promise for spin-off terrestrial applications of great importance including drinking water treatment, wastewater treatment, and waste stream reduction. While rotating RO has been investigated to recycle the wastewater in a spacecraft [27-30,57,58], prevent scale formation in water softening [25,59], and control biofouling on RO membranes [60], the technology is still in its early stages of development because of its complex hydrodynamic characteristics and lack of information on the design and operation. Substantial work is necessary to understand the physics underlying rotating RO and broaden its application for water and wastewater treatment.

References

1. B. V. d. Bruggen and C. Vandecasteele, "Distillation vs. membrane filtration: overview of process evolutions in seawater desalination". *Desalination*, **143,** 207-218 (2002).
2. H. F. Ridgeway, *Reverse osmosis technology: applicaitons for high-purity water production.* Marcel Dekker (1988).
3. D. Paul and K. Ohlrogge, "Membrane separation processes for clean production". *Environ. Progress*, **17,** 137-145 (1998).
4. D. J. Demboski, J. H. Benson, G. E. Rossi, N. S. Leavitt, and M. A. Mull, "Evolution in U.S. navy shipboard sewage and graywater programs". *Proceedings of the ASNE Environmental Symposium "Environmental Stewardship: Ships and Shorelines,"* November 1997 (1997).
5. R. J. Ray, S. B. McCray, and D. D. Newbold, "Small-scale membrane systems for the recovery and purification of water". *Sep. Sci. Tech.*, **26,** 1155-1176 (1991).
6. E. Matthiasson and B. Sivik, "Concentration polarization and fouling". *Desalination*, **35,** 59-103 (1980).
7. U. Merin and M. Cheryan, "Factors effecting the mechanism of flux decline during ultrafiltration of cottage cheese whey". *J. Food Proc.*, **4,** 183-198

(1980).
8. W. F. Blatt, A. Dravid, A. S. Michaels, and L. Nelson, *Membrane Science and Technology*. Plenum Press (1970).
9. T. J. Kennedy, R. L. Merson, and B. J. McCoy, "Improving permeation flux by pulsed reverse osmosis". *Chem. Eng. Sci.*, **29,** 1927-1931 (1974).
10. K. Y. Chung, W. A. Edelstein, and G. Belfort, "Dean vortices with wall flux in a curved channel membrane system. 6. Two dimensional magnetic resonance imaging of the velocity field in a curved impermeable slit". *J. Membrane Sci*, **81,** 151-162 (1993).
11. K.-Y. Chung, W. A. Edelstein, X. Li, and G. Belfort, "Dean vortices in a curved channel membrane system: 5 Three dimensional magnetic resonance imaging and numerical analysis of the velocity field in a curved impermeable tube". *AIChE J.*, **39,** 1592-1602 (1993).
12. J. Engler and M. R. Wiesner, "Particle fouling of a rotating membrane disk". *Water Res.*, **34,** 557-565 (2000).
13. T. Murase, E. Iritani, P. Chidphong, K. Kano, K. Atsumi, and M. Shirato, "High-speed microfiltration using a rotating cylinderical ceramic Membrane". *Ind. Chem. Eng.*, **31,** 370-378 (1991).
14. R. M. Lueptow, "Fluid mechanics of a rotating filter separator". *American Filtration and Separation Society*, Northport, AL, USA, (1995).
15. G. Belfort, J. M. Pimbley, A. Greiner, and K. Y. Chung, "Diagnosis of membrane fouling using a rotating annular filter. 1. Cell culture media". *J. Membrane Sci*, **77,** 1-22 (1993).
16. G. Belfort, P. Mikulasek, J. M. Pimbley, and K. Y. Chung, "Diagnosis of membrane fouling using a rotating annular filter. 2. Dilute particle suspensions of know particle size". *J. Membrane Sci.*, **77,** 23-39 (1993).
17. U. B. Holeschovsky and C. L. Cooney, "Quantitative description of ultrafiltration in a rotating filtration device". *AIChE J.*, **37,** 1219-1226 (1991).
18. L. J. Zeman and A. L. Zydney, *Microfiltration and Ultrafiltration: Principles and Applications*. Marcel Dekker, Inc. (1996).
19. P. Perseghin, A. Pagani, P. M. Fornasari, and L. Salvaneschi, "Doonor Plasmapheresis: A Comparative Study Using Four Different Types of Equipment". *Int. J. Artificail Organs*, **10,** 51-56 (1987).
20. H. Fischel and W. F. McLaughlin, Blood Fractionation System and Method. *US Patent*, 5,034,135 (1991).
21. K. H. Kroner and V. Nissinen, "Dynamic filtration of microbial suspensions using an axially rotating filter". *J. Membrane Sci*, **36,** 85-100 (1988).
22. S. Lee and R. M. Lueptow, "Rotating reverse osmosis system based on Taylor-Couette flow". *12th International Couette Taylor Workshop*, Evanston, IL, U.S.A., September, (2001).
23. S. Lee and R. M. Lueptow, "Rotating reverse osmosis: a dynamic model for flux and rejection". *J. Membrane Sci*, **192,** 129-143 (2001).
24. S. Lee and R. M. Lueptow, "Experimental Verification of a Model for Rotating Reverse Osmosis". *Desalination*, **146,** 353-359 (2002).
25. S. Lee and R. M. Lueptow, "Control of Scale Formation in Reverse Osmosis by Membrane Rotation". *Desalination*, **155,** 131-139 (2003).
26. S. Lee and R. M. Lueptow, "Model predictions and experiments for rotating reverse osmosis for space missions water reuse". *Sep. Sci. Tech., in press* (2003).
27. R. M. Lueptow, "Rotating Membrane Water Purification for Long-Term Human Presence in Space". Final Report, Final Report Grant # NAG 9-1053 (2002).
28. R. M. Lueptow, "Rotating Membrane Water Purification for Long-Term Human Presence in Space". Research Proposal, Grant # NAG 9-1053 (1999).
29. R. M. Lueptow, "Advancing Rotating Membrane Water Purification for Human Life Support in

Space". Research Proposal, Grant # NAG 9-1053 (2002).
30. S. Lee and R. M. Lueptow, "Rotating Membrane Water Purification for Long-Term Human Presence in Space", *Bioastronautics Investigators Workshop 2001*, Galveston, Texas, USA, January 17-19, (2001).
31. G. I. Taylor, "Stability of a viscous liquid contained between two rotating cylinders". *Phil. Trans. A*, **223,** 289-343 (1923).
32. S. Chandrasekhar, *Hydrodynamic and Hydromagnetic Stability*. Oxford University Press (1961).
33. R. C. DiPrima, "The stability of a viscous fluid between rotating cylinders with an axial flow". *J. Fluid Mech.*, **9,** 621-631 (1969).
34. K. Kataoka, H. Doi, and T. Komai, "Heat/mass transfer in Taylor vortex flow with constant axial flow rates". *Int. J. Heat Mass Transfer*, **20,** 57-67 (1977).
35. E. L. Koschmieder, *Benard Cell and Taylor Vortices*. Cambridge University Press (1993).
36. A. Rectenwald, M. Lucke, and H. W. Muller, "Taylor vortex formation in axial through-flow: Linear and weakly nonlinear analysis". *Phys. Rev. E*, **48,** 4444-4454 (1993).
37. R. C. DiPrima and A. Pridor, "The stability of viscous flow between rotating concentric cylinders with an axial flow". *Proc. R. Soc. Lond. A*, **366,** 555-573 (1979).
38. K. Min and R. M. Lueptow, "Circular Couette-Flow with Pressure-Driven Axial-Flow and a Porous Inner Cylinder". *Exp. Fluids*, **17,** 190-197 (1994).
39. K. Min and R. M. Lueptow, "Hydrodynamic Stability of Viscous-Flow between Rotating Porous Cylinders with Radial Flow". *Phys. Fluids*, **6,** 144-151 (1994).
40. M. Lopez-Leiva, *Ultrafiltration in rotary annular flow*, University of Lund (1979).
41. C. K. Choi, J. Y. Park, P. W.C., and J. J. Kim, "A study on dynamic separation of silica slurry using a rotating membrane filter: 2. Modelling of cake formation". *J. Membrane Sci*, **157,** 177-187 (1999).
42. J. Y. Park, C. K. Choi, and J. J. Kim, "A study on dynamic separation of silica slurry using a rotating membrane filter: 1. Experiments and filtrate fluxes". *J. Membrane Sci*, **97,** 263-273 (1994).
43. S. T. Wereley, A. Akonur, and R. M. Lueptow, "Particle-fluid velocities and fouling in rotating filtration of a suspension". *Journal of Membrane Science*, **209,** 469-484 (2002).
44. A. Akonur and R. M. Lueptow, "Chaotic mixing and transport in wavy Taylor Couette flow". *Physica D*, **167,** 183-196 (2002).
45. J. Schwille, D. Mitra, and R. M. Lueptow, "Design parameters for rotating cylindrical filtration". *J. Membrane Sci*, **204,** 53-65 (2002).
46. W. S. W. Ho and K. K. Sirkar, *Membrane Handbook*. Van Nostrand Reinhold (1992).
47. M. Cheryan, *Ultrafiltration and Microfiltration Handbook*. Technomic Publishing Company, Inc (1998).
48. G. Baier, *Liquid-liquid extraction based on a new flow pattern: two fluid Taylor-Couette flow computational fluid dynamics*, Chemical Engineering, University of Wisconsin, USA (1999).
49. G. Baier, T. M. Grateful, M. D. Graham, and E. N. Lightfoot, "Prediction of mass transfer in spatially periodic systems". *Chem. Eng. Sci.*, **54,** 343-355 (1999).
50. S. Lee and R. M. Lueptow, "Mass Transfer in Rotating Reverse Osmosis Based on Couette-Taylor Flow". *13th International Couette-Taylor Workshop*, Barcelona, Spain, July 3-5, (2003).
51. T. Mizushina, "The electrochemical method in transport phenomena". *Adv. Heat Transfer*, **7,** 87-100 (1971).
52. F. Coeuret and J. Legrand, "Mass transfer at the electrodes of concentric cylindrical reactors combining axial flow and rotation of the inner cylinder". *Elecrochimica Acta*, **26,** 865-872 (1981).

53. Y. Kawase and J. J. Ulbrecht, "Laminar mass transfer between concentric rotating cylinders in the presence of Taylor vortices". *Electrochimica Acta*, **33,** 199-203 (1988).
54. V. L. Snoeyink and D. Jenkins, *Water Chemistry*. John Wiley & Sons, Inc (1980).
55. R. M. Lueptow and S. Lee, "Rotating reverse osmosis for wastewater recovery in manned space missions". *17th Annual Meeting of American Society for Gravitational and Space Biology*, Alexandria, VA, USA, November 7-10, (2001).
56. S. Lee and R. M. Lueptow, "Rotating Reverse Osmosis: Effect of Operating Conditions". *AIChE 2002 Annual Meeting*, Indianapolis, Indiana, USA, Nov. 3-8, (2002).
57. S. Lee and R. M. Lueptow, "Space Mission Wastewater Recovery System Using Rotating Reverse Osmosis: Process Simulation". *32nd International Conference on Environmental Systems (ICES)*, San Antonio, Texas, USA, July 15-18, (2002).
58. S. Lee and R. M. Lueptow, "Rotating reverse osmosis filtration for space missions". *Science and Technology of Filtration and Separation for the 21st Century*, Tampa, Florida, USA, MAY 1-4, (2001).
59. S. Lee and R. M. Lueptow, "A novel RO membrane technique based on Taylor-Couette flow for scale control in water desalination". *AWWA Membrane Conference*, Atlanta, USA, Mar. 3-5, (2003).
60. R. M. Lueptow and K. Gray, "Nanoparticle Photocatalysis to Prevent Biofouling". Research proposal to NSF, (2003).
61. J. Grifoll, X. Farriol, and F. Giralt, "Mass transfer at smooth and rough Surfaces in a circular Couette flow". *Int. J. Heat Mass Transfer*, **29 (12),** 1911-1918 (1986).
62. J. Legrand, P. Dumargue, and F. Coeuret, "Overall mas transfer to the rotating inner electrode of a concentric cylindrical reactor with axial flow". *Electrochimica Acta*, **25,** 669-673 (1980).
63. M. Eienberg, C. W. Tobias, and C. R. Wilke, "Mass transfer at rotating cylinders". *Chem. Eng. Prog. Symp. Ser.*, **51,** 1-16 (1955).
64. J. R. Flower, N. Macleod, and A. P. Shahbenderian, "The Radial Transfer of Ma and Momentum in an Axial Fluid Stream between Coaxial Rotating Cylinders -I Experimental Measurement". *Chem. Eng. Sci.*, **24,** 637-650 (1969).
65. N. Macleod and T. Rue, "The radial transfer of mass to an axial stream of liquid between coaxial rotating cylinders". *Chem. Eng. Sci.*, **30,** 235-242 (1975).
66. S. Cohen and D. M. Marom, "Experimental and theoretical study of a rotating annular flow reactor". *Chem. Eng. J.*, **27,** 87-97 (1983).
67. A. B. Strong and L. Carlucci, "An Experimental Study of Ma Transfer in Rotating Couette Flow with Low Axial Reynolds number." *Can. J. Chem. Eng.*, **54,** 295-299 (1976).